HIGHLIGHTS

Zinc binds to TPPP/p25 coupled with its dimerization and enhanced tubulin polymerization activity.
The intracellular level of TPPP/p25, a microtubule associated protein, is enhanced by zinc uptake.
Zinc-induced structural change inhibits the degradation of TPPP/p25 by the proteasome.
This effect occurs in cells expressing TPPP/p25 ectopically or endogenously at different levels.

ZINC-INDUCED STRUCTURAL CHANGES OF THE DISORDERED TPPP/p25 INHIBITS ITS DEGRADATION BY THE PROTEASOME

Attila Lehotzky[a*], Judit Oláh[a*], Sándor Szunyogh[a], Adél Szabó[a], Tímea Berki[b], Judit Ovádi[a§]

[a]Institute of Enzymology, Research Centre for Natural Sciences, Hungarian Academy of Sciences, Budapest, Hungary; [b]Department of Immunology and Biotechnology, Medical School, University of Pécs, Pécs, Hungary

*These authors contributed equally to this work.

[§]Address correspondence to: Judit Ovádi, Institute of Enzymology, Research Centre for Natural Sciences, Hungarian Academy of Sciences, Budapest, Magyar tudósok körútja 2., H-1117, Hungary, Tel. (36-1) 3826-714; E-mail: ovadi.judit@ttk.mta.hu

E-mail addresses:
AL: lehotzky.attila@ttk.mta.hu;
J. Oláh: olah.judit@ttk.mta.hu;
SSZ: szunyogh.sandor@ttk.mta.hu;
ASZ: szaboadel90@gmail.com;
TB: timea.berki@aok.pte.hu;
J. Ovádi: ovadi.judit@ttk.mta.hu;

ABSTRACT

Tubulin Polymerization Promoting Protein/p25 (TPPP/p25), a neomorphic moonlighting protein displaying both physiological and pathological functions, plays a crucial role in the differentiation of the zinc-rich oligodendrocytes, the major constituent of myelin sheath; and it is enriched and co-localizes with α-synuclein in brain inclusions hallmarking Parkinson's disease and other synucleinopathies. In this work we showed that the binding of Zn^{2+} to TPPP/p25 promotes its dimerization resulting in increased tubulin polymerization promoting activity. We also demonstrated that the Zn^{2+} increases the intracellular TPPP/p25 level resulting in a more decorated microtubule network in CHO10 and CG-4 cells expressing TPPP/p25 ectopically and endogenously, respectively. This stabilization effect is crucial for the differentiation and aggresome formation under physiological and pathological conditions, respectively. The Zn^{2+}-mediated effect was similar to that produced by treatment of the cells with MG132, a proteasome inhibitor or Zn^{2+} plus MG132 as quantified by cellular ELISA. The enhancing effect of zinc ion on the level of TPPP/p25 was independent of the expression level of the protein produced by doxycycline induction at different levels or inhibition of the protein synthesis by cycloheximide. Thus, we suggest that the zinc as a specific divalent cation could be involved in the fine-tuning of the physiological TPPP/p25 level counteracting both the enrichment and the lack of this protein leading to distinct central nervous system diseases.

KEYWORDS

Tubulin Polymerization Promoting Protein/p25, zinc, oligodendrocyte

HIGHLIGHTS

Zinc binds to TPPP/p25 coupled with its dimerization and enhanced tubulin polymerization activity.
The intracellular level of TPPP/p25, a microtubule associated protein, is enhanced by zinc uptake.
Zinc-induced structural change inhibits the degradation of TPPP/p25 by the proteasome.
This effect occurs in cells expressing TPPP/p25 ectopically or endogenously at different levels.

1. INTRODUCTION

Zinc is a ubiquitous and essential micronutrient for microorganisms, plants, animals and humans and is intimately linked to health, well-being as well as a number of disease states [1-5]. Zinc is involved in an extraordinary range of biological functions and is essential for growth, development and for a host of diseases, although its precise role is not fully understood. The total intracellular Zn^{2+} concentration in eukaryotic cells is approximately 200 μM, while its intracellular free concentration is in the nanomolar range [6]. Inside the cells, most of the divalent Zn^{2+} cation is bound to specific Zn^{2+} transporters and delivered to specific targets. Thus zinc transporters and zinc binding proteins play crucial roles in zinc homeostasis and maintenance of a very narrow range of intracellular free zinc concentration, which is optimal for cellular functions [7-9]. A number of data have been reported which indicate compartments in the tissues with accumulated zinc concentration, for example, in the myelin membrane [10-11] and the synaptic vesicles of some neurons in the brain [12] where the Zn^{2+} concentration is about 50 µM and 1 mM, respectively (for review see [3]). In fact, the brain has the highest zinc concentration as compared to other organs; Zn^{2+} can modulate the activity of neurotransmitter receptors thus may play a potential neuromodulatory role [12]. In myelinating oligodendrocytes, Zn^{2+}-myelin basic protein and Zn^{2+}-proteolipid protein complexes are reported to be essential for maintaining the integrity of the myelin sheath [13-15]. In animals, zinc-deficiency results in loss of compact myelin [16-17]. The excessive Zn^{2+} release plays a key role in inducing neuronal death during central nervous system (CNS) injury. Dyshomeostasis of zinc ions has been observed in the case of different neurodegenerative diseases such as Alzheimer's and Parkinson's diseases; moreover, zinc ions accelerate the aggregation/fibrillization of alpha-synuclein, hallmark protein of Parkinson's disease [18-19].

Tubulin Polymerization Promoting Protein/p25 (TPPP/p25) modulates the dynamics and stability of the microtubule system [20] and plays a crucial role in the differentiation of the oligodendrocytes thus likely in the ensheathment of axons as well [21-22]. TPPP/p25 does not have a well-defined 3D structure; it is an *intrinsically disordered* protein that is involved in the etiology of distinct CNS diseases such as multiple sclerosis, oligodendroglioma and synucleinopathies [23-25]. TPPP/p25 is a prototype of neomorphic moonlighting proteins which display distinct physiological and pathological functions by interacting with distinct protein partners [26]. TPPP/p25 occurs both in monomeric and homodimeric forms, the dimer has been found to be more compact as expected from the assembly of the highly disordered monomers [27]. The protein has a zinc finger motif (His_2Cys_2) (His61-Cys83) within its flexible core region which is straddled by extended unstructured N- and C-terminal segments [28-29]. The binding of Zn^{2+} to TPPP/p25 induces molten globule formation, but not a well-defined tertiary structure [29]. The affinity constant of zinc binding to TPPP/p25 was evaluated from isothermal titration calorimetry, Ka = $(3.29 \pm 0.64) * 10^4 M^{-1}$ [29]. Zn^{2+} of the divalent cations can uniquely influence the physiologically relevant functions of TPPP/p25 such as its tubulin polymerization promoting and GTPase activities.

In this work we showed that the enhanced tubulin polymerization promoting activity of TPPP/p25 in the presence of zinc is resulted from the oligomerization of the monomeric TPPP/p25. In CHO10 and CG-4 cells treated with additional Zn^{2+} the TPPP/p25 level significantly increased primarily due to the zinc-mediated stabilization against the degradation of the protein by the proteasome system. The effect of zinc on TPPP/p25 level was similar at different intracellular milieu produced by inhibition of either protein synthesis or the proteasome machinery.

2. MATERIALS AND METHODS

2.1 Protein purification

The coding sequence of TPPP/p25 was obtained by polymerase chain reaction using the pEGFP-TPPP/p25 plasmid [30] as template and the primers 5′-ATACATATGGCTGACAAGG-3′ and 5′-GATAAGCTTCTACTTGCCCCCTTG-3′. The polymerase chain reaction fragment was digested with NdeI and HindIII and cloned between the appropriate restriction sites of the pT7-7 vector (Stanley Tabor, Harvard Medical School, Boston, Massachusetts; [31]; http://www.currentprotocols.com/WileyCDA/CPUnit/refId-mb1602.html), resulting in the pT7-7-TPPP/p25 plasmid. The protein was expressed in E coli, and then the cells were centrifuged at 2500 g at 4 °C for 20 min. Next the cells were suspended in 10 mM phosphate buffer pH 7.0 containing 200 mM NaCl and protease inhibitors (1 μg/mL leupeptin, 1 μg/mL pepstatin, 10 μM 4-(2-aminoethyl) benzenesulfonyl fluoride and 1 mM benzamidine). After sonication and further centrifugation at 50000 g at 4 °C for 25 min, the extract was dialyzed against buffer A (10 mM phosphate, pH 7.0), then chromatographed on SP Sephadex ion-exchange column with a linear NaCl gradient from 0 to 1 M in buffer A. TPPP/p25 eluted at 0.3 M NaCl, it was dialyzed against 50 mM ammonium acetate and lyophilized. Purity of prepared TPPP/p25 was checked by sodium dodecyl sulfate polyacrylamide gel electrophoresis (SDS-PAGE).

Monoclonal anti-TPPP/p25 antibody (mAb clone No. 6/C10) was labeled with (+)-Biotin-N-hydroxysuccinimide ester (NHS-D-Biotin, Sigma H1759) according to the manufacturer's instructions and [32]. Briefly, the Protein G affinity purified antibody was dialyzed against 0.1 M sodium carbonate buffer pH 8.4 containing 0.1% NaN_3 at 4 °C. After dialysis, the protein concentration was adjusted to 20 mg/mL. The NHS-D-Biotin was dissolved in dimethyl sulfoxide immediately prior to use (solution was protected from light) at a concentration of 22 mg/mL. Using a volume equal to 10% of the total volume of the immunoglobulin solution, the NHS-D-Biotin was added to the immunoglobulin solution with gentle stirring, and incubated at room temperature for 4 hours. Finally the reaction solution was dialyzed against several changes of phosphate buffered saline (PBS) buffer (0.01 M sodium phosphate, 0.15 M sodium chloride, pH 7.4) containing 0.1% NaN_3 at 4 °C.

Tubulin was purified from bovine brain by the method of Na and Timasheff [33].

2.2 Fluorescence spectroscopy

A 10 mM stock solution of N-(6-methoxy-8-quinolyl)-p-toluenesulfonamide (TSQ) (Invitrogen) was prepared in dimethyl sulfoxide. The spectrum of 20 μM TSQ without or with 5 μM $ZnCl_2$ and 5 μM TPPP/p25 was measured at room temperature in PBS buffer, pH 7.2. A $MnCl_2$ solution of 5 μM was added to the TSQ-$ZnCl_2$-TPPP/p25 sample, where indicated. The fluorescence spectra were recorded in quartz cuvettes of 1 cm optical path length at 25 °C by a FluoroMax-3 spectrofluorometer (Jobin Yvon Inc., Longiumeau, France). The excitation wavelength was 360 nm (slit width 4 nm), emission spectra were collected from 400 to 600 nm (slit width 4 nm). Data were processed using DataMax software. Scanning was repeated three times, and the spectra were averaged.

2.3 Turbidity measurements

The assembly of 7 μM tubulin was assessed in polymerization buffer (50 mM 2-(N-morpholino)ethanesulfonic acid buffer) pH 6.6 containing 100 mM KCl, 1 mM dithioerythritol (DTE), 1 mM $MgCl_2$ and 1 mM ethylene glycol tetraacetic acid) at 37 °C. The polymerization of tubulin was induced by addition of 3 μM TPPP/p25 in the absence and presence of 100 μM $ZnCl_2$. In one case a TPPP/p25 stock solution at ~100-fold higher concentration (400 μM) as in the assay was added to the tubulin diluted in the cuvette without or with $ZnCl_2$; in the other case TPPP/p25 was diluted into the cuvette with or without $ZnCl_2$, incubated for 10 minutes and the polymerization was initiated by stock solution of tubulin. The turbidity was monitored at 350 nm by a Cary 100 spectrophotometer (Varian, Walnut Creek, Australia).

2.4 Cell Culture and Manipulation

CHO10 cells originated from CHO Tet-On cell line were induced to express human TPPP/p25 as described previously [34]. Cells were grown on 12 mm diameter coverslips for microscopic analysis (1 x 10^4 cells) and on 24-well plates for immunoblotting (2.5 x 10^4 cells). For cellular enzyme-linked immunosorbent assay (cELISA), cells were plated on 96-well plates and cultured overnight with doxycycline, as indicated.

In the experiments where indicated, a 10 μM solution of MG132 (Sigma) or $ZnCl_2$ (Sigma) (from 10 mM stock solution dissolved in sterile ultrapure water) was added for 3 hours, then 1 μM vinblastine (Sigma) was added to the assay at the last hour of the induction period. In the case of the inhibition of protein synthesis, 20 μg/mL cycloheximide was added to the cells (three hours and five minutes incubation) five minutes before the addition of $ZnCl_2$ and/or MG132, where indicated. The CG-4 cell line was propagated in DMEM-N1 30% conditioned medium obtained by neuroblastoma cell line B104 as described previously [22, 35]. For immunofluorescence microscopy, 2 x 10^4 cells were plated onto poly-L-ornithine-coated glass coverslips, and the cells were incubated for 3 hours with 1 μM $ZnCl_2$, (from 1 mM stock solution in sterile ultrapure water), where indicated.

2.5 ELISA

cELISA: Cells after manipulation on tissue culture plate were fixed by ice cold methanol for 10 minutes. Next the wells were rehydrated by PBS, and blocked with 1 mg/mL bovine serum albumin (BSA) in PBS containing 0.1% Triton-X-100 for 1 h at room temperature. Then the plate was sequentially incubated with monoclonal anti-TPPP/p25 antibody (1.5 μg/mL) [23] and with an anti-mouse IgG-peroxidase conjugate (1:2500, Sigma) in PBS buffer containing 1 mg/mL BSA and 0.1% Triton-X-100, and incubated for 1 h at room temperature (both in a volume of 50 μL). Following each incubation steps the wells were washed thrice with PBS for 5 min. The TPPP/p25 concentration was quantified by peroxidase conjugated antibody using o-phenylenediamine in the concentration of 3.7 mM with 0.03% peroxide as substrate. The reaction was stopped after 15 min with 1 M H_2SO_4; absorbance was read at 490 nm with an EnSpire Multimode Reader (Perkin Elmer).

Sandwich ELISA: The plate was coated with 1 μg/mL (50 μL/well) monoclonal anti-TPPP/p25 antibody [23] in 200 mM Na_2CO_3 buffer pH 9.6 overnight at 4 °C. The wells were blocked with 1 mg/mL BSA in PBS for 1 h at room temperature. Next, the plate was incubated with serial dilutions of 5 μM TPPP/p25 for 1 h at room temperature in PBS. Where indicated, TPPP/p25 was pre-incubated with 2 or 10 μM divalent metal ions and/or 100 μM DTE for 30 min at room temperature. Then the plate was sequentially incubated with biotinylated monoclonal anti-TPPP/p25 antibody (1 μg/mL) and peroxidase conjugated avidin (Calbiochem) (2.5 μg/mL). Both antibodies were in PBS buffer containing 1 mg/mL BSA, and incubated for 1 h at room temperature. Between each incubation step the wells were washed thrice with PBS containing 0.05% Tween 20 for 10 min. The presence of antibodies was detected using o-phenylenediamine as described at the cELISA section.

2.6 Immunocytochemistry

CHO10 cells were fixed with ice-cold methanol for 10 minutes. After washes in PBS, samples were blocked for 30 minutes in PBS-0.1% Triton X-100 (TPB) containing 5% fetal calf serum (TPB-FCS). Subsequently, the cells were stained with a monoclonal anti-TPPP/p25 antibody (1 μg/mL) [23] followed by Alexa 546 conjugated anti-mouse antibody (2 μg/mL) (Invitrogen). The samples were washed three times with PBS after antibody incubation. Nuclei were counterstained with 4,6-diamidino-2-phenylindole (DAPI). CG-4 cells were fixed and blocked similarly as in the case of CHO10 cells. Subsequently, the cells were stained with a monoclonal antibody against α-tubulin (clone DM1A, Sigma) (1 μg/mL) and a polyclonal rat serum against TPPP/p25 (1:1000) [25] followed by Alexa 488 and Alexa 546 conjugated anti-mouse (1 μg/mL) and anti-rat (1 μg/mL) antibodies, respectively (both from Invitrogen and cross-absorbed). Images of cell samples were acquired on a Leica DMLS microscope or on a Zeiss LSM710 confocal microscope.

2.7 Immunoblotting

For detection of TPPP/p25 level in cellular samples, wells were washed with PBS, next the cells were lysed in 150 μL RIPA buffer containing protein inhibitor mix (Sigma). Samples were centrifuged at

10000 g at 4°C for 10 minutes and the supernatants were stored at -70 °C. The protein concentration of samples was measured by the Bradford method [36] using the Bio-Rad protein assay kit. 10 µg of extracts were analyzed by SDS-PAGE and immunoblotting onto polyvinylidene difluoride membrane using a polyclonal rat serum against TPPP/p25 (1:5000) [25] and a monoclonal antibody against glyceraldehyde-3-phosphate dehydrogenase (GAPDH) (1 µg/mL) (CB1001, 6C5, Calbiochem), followed by an anti-rat and anti-mouse IgG-peroxidase conjugate, respectively (both 1:5000, Sigma).

3. RESULTS

3.1.1 Specific binding of zinc to TPPP/p25

A commonly used fluorophore, TSQ, forms a 2:1 complex with Zn^{2+} in a reaction that results in a dramatic increase of the fluorescence emission spectrum accompanied by a shift of the maximum; it also can form a ternary TSQ-zinc-protein complex with different emission maximum [37]. TSQ is used as a zinc-specific fluorescent chelator in spite of the fact that it chelates a variety of transition metal cations with varying affinities; however, it fluoresces strongly in complex with zinc and only weakly with other metals of atomic radii similar to zinc. In order to confirm the direct and specific binding of Zn^{2+} to TPPP/p25 fluorescence spectroscopic studies were carried out with TSQ sensor. As shown in Fig. 1A, TPPP/p25 increased the fluorescence intensity of the TSQ-zinc complex coupled with a blue-shift indicating the binding of zinc complex to TPPP/p25. This finding supports our previous data obtained with 8-anilinonaphthalene-1-sulfonic acid [29]. Now the specificity of the zinc binding was tested by using manganese, another divalent cation, which did not affect the spectrum.

3.1.2 Zinc-induced functional changes of TPPP/p25

Previously we reported that the zinc-induced structural alteration affected the tubulin polymerization promoting activity of TPPP/p25 [29]. Later on, we have also demonstrated by size exclusion gel chromatography that TPPP/p25 displays concentration-dependent dimerization which affects its tubulin polymerization promoting activity [27], however, the relationship of these processes was not studied.

Here we analyzed the functional consequences of zinc binding to TPPP/p25 by means of turbidity assay at different pre-incubation conditions: i) TPPP/p25 solution was added to the tubulin diluted in the cuvette with or without zinc; ii) the cuvette contained the diluted TPPP/p25 with or without zinc, and the reaction was initiated by tubulin from a stock solution. At all these conditions the concentrations of tubulin, TPPP/p25 and $ZnCl_2$ were identical in all turbidity assays. We demonstrated earlier that the zinc cation did not influence tubulin polymerization in the absence of TPPP/p25 when polymerization was induced by paclitaxel or TPPP3/p20, a TPPP/p25 homologue without zinc finger motif [29].

As illustrated in Fig. 1B, the potency of TPPP/p25 to promote tubulin polymerization was much higher when the polymerization was initiated by TPPP/p25 from the stock solution than by tubulin (when TPPP/p25 was diluted) as expected [27]. The addition of zinc counteracted the dilution-mediated reduction

of its tubulin polymerization activity. This finding shows that the TPPP/p25 species mediating tubulin assembly is activated by the addition of zinc. Since the result of the control experiment (no zinc) suggested that the dimer enriched TPPP/p25 sample displayed much higher polymerization activity, it is likely that the zinc favors the dimerization of TPPP/p25.

3.1.3 Zinc-induced dimerization of TPPP/p25

To obtain evidence on the role of zinc in the dimerization of TPPP/p25, sandwich ELISA experiment was performed. The rational of this study was as follows. Monoclonal anti-TPPP/p25 antibody was immobilized on the plate, and TPPP/p25 pre-incubated or not with $ZnCl_2$ was diluted onto the plate. Then the same monoclonal anti-TPPP/p25 antibody in biotinylated form was added onto the plate, the binding of which to the dimeric TPPP/p25 could be detected through peroxidase conjugated avidin reaction. This sandwich ELISA arrangement ensured the exclusive detection of the dimer/oligomer TPPP/p25 species since monomers cannot bind simultaneously to the immobilized and the biotinylated antibodies with the same epitope as was demonstrated for alpha-synuclein [38] and beta-amyloid systems [39] as well.

Serial dilution of TPPP/p25 was added onto the plate without or with $ZnCl_2$. The 5 μM TPPP/p25 solutions were prepared at three different manners: i) TPPP/p25 from a stock solution (400 μM) was diluted to 5 μM and added immediately onto the plate with or without $ZnCl_2$ or $MnCl_2$; ii) 5 μM TPPP/p25 incubated at room temperature for 30 min, or iii) 5 μM TPPP/p25 incubated with or without $ZnCl_2$ at room temperature for 30 min in the presence of 100 μM DTE were added to the plates. The presence of Zn^{2+}, but not that of $MnCl_2$, increased the binding of the biotinylated TPPP/p25 antibody indicating the elevation of the amount of dimeric/oligomeric forms (Fig. 1C and D). The effect was more pronounced at 10 μM as compared to that at 2 μM Zn^{2+}. This finding shows the specific effect of the zinc on the oligomerization of TPPP/p25. The dilution of TPPP/p25 followed by 30 min incubation reduced the amount of dimeric (oligomeric) forms in the diluted sample (Fig. 1C). This effect was more pronounced in the presence of DTE when the oligomers were not stabilized by intermolecular S-S bridges (Fig 1C and D). In fact, the presence of DTE diminished the disulfide bridges formed by spontaneous oxidation during the incubation at room temperature as we described previously [27]. Consequently, in the diluted protein sample the presence of DTE resulted in predominantly monomers which display no or very low binding affinity. The presence of zinc, however, counteracted this effect; this divalent metal ion increased the amount of dimeric/oligomeric forms and diminished the effect of dilution. These data show that, on one hand, a significant fraction of TPPP/p25 occurs in dimeric form in the stock solution and it is partially stabilized by intermolecular disulfide bridges, on the other hand, the zinc-mediated effect at relatively high TPPP/p25 concentration is less pronounced since the major part of the disordered protein is in dimeric form even in the absence of zinc.

Therefore, the *in vitro* data obtained with human recombinant TPPP/p25 underline the crucial role of the divalent zinc cation in the formation/stabilization of the dimeric form which has been proposed to be the physiologically relevant species [29]. As we documented previously neither the structural nor the

functional effects induced by Zn^{2+} was detected by other cations such as Ca^{2+} and Al^{3+} [29]. This issue is now supported by control data obtained with Mn^{2+} in both TSQ and sandwich ELISA experiments (cf. Fig. 1A and C).

3.2.1 Zinc-induced enhancement of the intracellular TPPP/p25 level

In order to visualize the zinc-induced alterations at cell level, the intracellular TPPP/p25 concentration was analyzed in *vivo* with CHO10 and CG-4 cell lines expressing TPPP/p25 ectopically and endogenously, respectively. While CHO10 cells express TPPP/p25 following doxycycline induction, in the CG-4 oligodendrocyte cells TPPP/p25 is expressed endogenously at low level in the progenitor cells and at high level in the differentiated cells. The rational of these studies was based on our early observation that the inhibition of the proteasome machinery by MG132 elevated the TPPP/p25 level in HeLa cells [40]; it was concluded that the intrinsically unstructured TPPP/p25 can be degraded by the proteasome [40-41]. Thus we were interested in how the zinc uptake from the medium affects the intracellular TPPP/p25 level.

CHO10 cells were induced by doxycycline to express TPPP/p25 ectopically at modest level, then they were grown in medium without or with 10 μM $ZnCl_2$ (3 hours) to analyze the effect of this short-term treatment. The TPPP/p25 level (red) was visualized by confocal fluorescence microscopy using anti-TPPP/p25 antibody for specific staining. Fig. 2 presents a global overview of the effect of zinc-treatment that suggests the elevation of total TPPP/p25 level.

Next, we characterized the zinc-mediated effect on the intracellular TPPP/p25 level at various circumstances which could occur at physiological and/or pathological conditions.

The microtubule network is the major target of TPPP/p25: it specifically co-localizes with the microtubule but not with the actin filament [40] and modulates its dynamics and stability by its acetylation enhancing and bundling activities [34]. To obtain information on the role of the microtubule network in the zinc-induced elevation of the intracellular TPPP/p25 level, CHO10 cells expressing TPPP/25 and uploaded by zinc were treated with vinblastine, a well-established anti-microtubule agent (Fig. 3A). In the case of the untreated cells (no zinc) the TPPP/p25 level was considered as a control; the uptake of zinc cation resulted in significant enhancement in the intracellular TPPP/p25 level which was aligned along the filamentous (microtubule) network. The vinblastine treatment caused the collapse of the microtubule network in the zinc-treated and untreated cells. However, the zinc-containing cells apparently maintained higher TPPP/p25 level than the control ones likely due to the zinc-induced structural changes, indicating the stabilizing effect of this cation. These effects were quantified by cELISA as shown in Fig. 3B. The data revealed that zinc increased the TPPP/p25 level in similar extent independently of the disassembly of the microtubule network, although the absolute concentration of TPPP/p25 was higher in the control sample than in the vinblastine-treated one (it was less degraded), therefore the zinc can elevate the decoration of the microtubule network by TPPP/p25.

Next, we studied how the intracellular expression level of TPPP/p25 influences the zinc-mediated stabilizing effect. In this set of experiments TPPP/p25 was expressed in CHO10 cells at different levels in

the absence and presence of 5 or 10 μM $ZnCl_2$ (Fig. 4). cELISA assays provided quantitative data for the effect of zinc (Fig. 4B). We found that zinc increased the TPPP/p25 level at all concentrations of doxycycline except the highest. At 2500 ng/mL doxycycline induction the TPPP/p25 level seems to reach the upper limit, thus it is not surprising that the zinc-induced TPPP/p25 level is similar. This phenomenon could be attributed to different regulatory mechanisms, some of them have been identified (post-transcriptional level by microRNA, protein level by proteasomal degradation) [40, 42].

In another set of experiments the protein synthesis was inhibited by cycloheximide [43, 44] in CHO cells expressing TPPP/p25 at modest level (cf. Fig. 4) and the effect of zinc treatment on TPPP/p25 level was determined. Fig. 5 shows that the level of TPPP/p25, but not of GAPDH, was reduced significantly, and the presence of zinc counteracted this reducing effect as detected by immunoblotting. Indeed, the addition of $ZnCl_2$ to the cycloheximide-treated cells increased the intracellular TPPP/p25 level compared to the untreated ones. GAPDH, the synthesis of which is not inhibited by cycloheximide during the incubation due to its relatively long half-line [45], was used as loading control. These data (see also Fig. 6 for cELISA) further confirm that the positive effect of zinc on the enhancement of the TPPP/p25 level manifests itself even at condition when protein synthesis is inhibited.

3.2.2 Zinc inhibits the proteasome-derived degradation of TPPP/p25

Our previous results proved that the inhibition of the proteasome machinery by MG132 results in the elevation of TPPP/p25 level, and suggest its degradation by the proteasome [40]. To further characterize the influence of the zinc-induced structural changes in relation to the proteasome-derived degradation of TPPP/p25, CHO10 cells expressing TPPP/p25 were treated with MG132 and/or $ZnCl_2$ in the absence and presence of cycloheximide, and the TPPP/p25 level was quantified by cELISA (Fig. 6). These data provided evidence that the Zn^{2+}-induced structural change can enhance the intracellular level of the disordered protein by inhibiting its proteasomal degradation. cELISA analysis rendered it also possible to determine the combined effect of zinc and MG132 and to compare it with the effect caused by MG132 alone. Since these data did not differ significantly, it can be concluded that the zinc-induced structural change of TPPP/p25, including the dimerization, protects the disordered protein against its proteolytic degradation by the proteasomal machinery.

The physiological relevance of the zinc effect on the intracellular level of TPPP/p25 was also tested in CG-4 cells expressing the disordered protein endogeneously. As we have reported recently, the TPPP/p25 level is very low in the dividing progenitor cells. However, in the course of differentiation the TPPP/p25 level is drastically increasing; the down-regulation of TPPP/p25 by siRNA or miR206 significantly impeded the differentiation of the progenitor cells [22]. Fig. 7 shows that, on one hand, TPPP/p25 is aligned along the microtubule network in the projections; on the other hand, the presence of zinc can enhance the intracellular TPPP/p25 level in progenitor cells which likely contribute to the extension of projections during the differentiation.

4. DISCUSSION

Zinc ion, the second most abundant trace element in the human body, is essential for the structural stability of a variety of proteins involved in transcription, protein trafficking and enzymatic reactions [1-2]. The intracellular free zinc concentration is usually in the nanomolar range; however, oligodendrocyte progenitor cells accumulate Zn^{2+}. In myelinating oligodendrocytes, where TPPP/p25 is endogenously expressed, the intracellular Zn^{2+} concentration has been found to be relatively high (50 μM) [10-11]. In our experiments the concentrations of the $ZnCl_2$ added to the medium of CHO10 and oligodendrocyte CG-4 cell lines for zinc uptake were 5-10 μM and 1-2 μM, respectively. Therefore, the effect of this divalent cation appears to be physiologically relevant as the plasma and CSF Zn^{2+} concentration (~10 μM and ~ 2 μM) are comparable with these values, respectively [46]. Previously we reported that TPPP/p25 is extensively expressed during the differentiation of the progenitor cells which is crucial for the maturation of the oligodendrocytes [22]. However, its lack or enrichment was detected in oligodendrocyte cells of human brain tissues in the cases of glioma and multiple system atrophy, respectively [24, 25]. Now we established that the zinc uptake by progenitor oligodendrocytes gently modifies the TPPP/p25 level coupled with an enhancement of decoration of the microtubule network which could contribute to the initiation of differentiation. The decoration of the microtubule network by TPPP/p25 with its bundling and acetylation enhancing activities resulting in the stabilization of the network is a significant factor in aggresome formation [34]. These results suggest that the structural rearrangement of TPPP/p25 caused by zinc binding to the zinc finger motive could be a potential factor in brain physiology to optimize the intracellular TPPP/p25 level according to its physiological function.

A couple of unfolded/misfolded proteins due to their extensive aggregation-prone features are involved in distinct neurological and other disorders; for example tau/β-amyloid and α-synuclein are hallmark proteins of Alzheimer's and Parkinson's diseases, respectively [47-49]. There are intracellular mechanisms which could eliminate these "unwanted" proteins such as the proteasoma machinery [50-52]. We established that the proteasomal degradation is the major, if not exclusive, system responsible for the elimination of the disordered TPPP/p25. The degradation of TPPP/p25 is inhibited by MG132, a well-established inhibitor of proteasome [50]. The stabilization of TPPP/p25 against the proteolytic degradation is resulted from the structural changes of this disordered protein coupled with dimerization which is essential for the extension of projections playing role in the maintenance of the stability of the myelin sheath in the CNS. Thus, we suggest that the zinc, as a specific divalent cation could be involved in the fine-tuning of the physiological TPPP/p25 level. This is an important issue since both the enrichment and the lack of this protein leads to CNS diseases such as multiple system atrophy [25] and glioma [24], respectively.

5. LIST OF ABBREVIATIONS USED

bovine serum albumin, BSA; central nervous system, CNS; 4,6-diamidino-2-phenylindole, DAPI; dithioerythritol, DTE; enzyme-linked immunosorbent assay, ELISA; glyceraldehyde-3-phosphate dehydrogenase, GAPDH; N-(6-methoxy-8-quinolyl)-p-toluenesulfoamide, TSQ; phosphate buffered saline, PBS; sodium dodecyl sulfate polyacrylamide gel electrophoresis, SDS-PAGE; Tubulin Polymerization Promoting Protein, TPPP/p25.

6. COMPETING INTERESTS

The authors declare no conflict of interest.

7. ACKNOWLEDGEMENTS

This work was supported by the European Commission [(DCI ALA/19.09.01/10/21526/ 245-297/ALFA 111(2010)29], European Concerted Research Action [COST Action TD0905]; Hungarian National Scientific Research Fund Grants OTKA T-101039 and Richter Gedeon Nyrt (4700147899) to J. Ovádi. The funding body had no role in design, collection, analysis and interpretation of data, or in the writing of the manuscript. We thank István Horváth for the preparation of pT7-7-TPPP/p25 plasmid.

8. REFERENCES

[1] J.M. Berg and Y. Shi, The galvanization of biology: a growing appreciation for the roles of zinc, Science 271 (1996) 1081-1085.

[2] W. Law, E.E. Kelland, P. Sharp and N.J. Toms, Characterisation of zinc uptake into rat cultured cerebrocortical oligodendrocyte progenitor cells, Neurosci Lett 352 (2003) 113-116.

[3] E. Mocchegiani, C. Bertoni-Freddari, F. Marcellini and M. Malavolta, Brain, aging and neurodegeneration: role of zinc ion availability, Prog Neurobiol 75 (2005) 367-390.

[4] M. Murakami and T. Hirano, Intracellular zinc homeostasis and zinc signaling, Cancer Sci 99 (2008) 1515-1522.

[5] W. Maret, Zinc and human disease, Met Ions Life Sci 13 (2013) 389-414.

[6] R.D. Palmiter and S.D. Findley, Cloning and functional characterization of a mammalian zinc transporter that confers resistance to zinc, Embo J 14 (1995) 639-649.

[7] S. Yamashita, C. Miyagi, T. Fukada, N. Kagara, Y.S. Che and T. Hirano, Zinc transporter LIVI controls epithelial-mesenchymal transition in zebrafish gastrula organizer, Nature 429 (2004) 298-302.

[8] T. Kambe, Y. Yamaguchi-Iwai, R. Sasaki and M. Nagao, Overview of mammalian zinc transporters, Cell Mol Life Sci 61 (2004) 49-68.

[9] R.A. Colvin, C.P. Fontaine, M. Laskowski and D. Thomas, Zn2+ transporters and Zn2+ homeostasis in neurons, Eur J Pharmacol 479 (2003) 171-185.

[10] G.V. Iyengar, K. Kasperek and L.E. Feinendegen, Retention of the metabolized trace elements in biological tissues following different drying procedures. I. Antimony, cobalt, iodine, mercury, selenium and zinc in rat tissues, Sci Total Environ 10 (1978) 1-16.

[11] J.Y. Koh, Zinc and disease of the brain, Mol Neurobiol 24 (2001) 99-106.

[12] C.J. Frederickson, S.W. Suh, D. Silva, C.J. Frederickson and R.B. Thompson, Importance of zinc in the central nervous system: the zinc-containing neuron, J Nutr 130 (2000) 1471S-1483S.

[13] C. Earl, A. Chantry, N. Mohammad and P. Glynn, Zinc ions stabilise the association of basic protein with brain myelin membranes, J Neurochem 51 (1988) 718-724.

[14] D. Tsang, Y.S. Tsang, W.K. Ho and R.N. Wong, Myelin basic protein is a zinc-binding protein in brain: possible role in myelin compaction, Neurochem Res 22 (1997) 811-819.

[15] C. Baran, G.S. Smith, V.V. Bamm, G. Harauz and J.S. Lee, Divalent cations induce a compaction of intrinsically disordered myelin basic protein, Biochem Biophys Res Commun 391 (2010) 224-229.

[16] H. Gong and T. Amemiya, Optic nerve changes in zinc-deficient rats, Exp Eye Res 72 (2001) 363-369.

[17] B. Unal, H. Tan, Z. Orbak, I. Kiki, M. Bilici, N. Bilici, H. Aslan and S. Kaplan, Morphological alterations produced by zinc deficiency in rat sciatic nerve: a histological, electron microscopic, and stereological study, Brain Res 1048 (2005) 228-234.

[18] B.R. Roberts, T.M. Ryan, A.I. Bush, C.L. Masters and J.A. Duce, The role of metallobiology and amyloid-beta peptides in Alzheimer's disease, J Neurochem 120 Suppl 1 (2012) 149-166.

[19] K. Jomova, D. Vondrakova, M. Lawson and M. Valko, Metals, oxidative stress and neurodegenerative disorders, Mol Cell Biochem 345 (2010) 91-104.

[20] E. Hlavanda, J. Kovács, J. Oláh, F. Orosz, K.F. Medzihradszky and J. Ovádi, Brain-specific p25 protein binds to tubulin and microtubules and induces aberrant microtubule assemblies at substoichiometric concentrations, Biochemistry 41 (2002) 8657-8664.

[21] M. Takahashi, K. Tomizawa, S.C. Fujita, K. Sato, T. Uchida and K. Imahori, A brain-specific protein p25 is localized and associated with oligodendrocytes, neuropil, and fiber-like structures of the CA hippocampal region in the rat brain, J. Neurochem. 60 (1993) 228-235.

[22] A. Lehotzky, P. Lau, N. Tőkési, N. Muja, L.D. Hudson and J. Ovádi, Tubulin polymerization-promoting protein (TPPP/p25) is critical for oligodendrocyte differentiation, Glia 58 (2010) 157-168.

[23] R. Hoftberger, S. Fink, F. Aboul-Enein, G. Botond, J. Oláh, T. Berki, J. Ovádi, H. Lassmann, H. Budka and G.G. Kovacs, Tubulin polymerization promoting protein (TPPP/p25) as a marker for oligodendroglial changes in multiple sclerosis, Glia 58 (2010) 1847-1857.

[24] M. Preusser, A. Lehotzky, H. Budka, J. Ovádi and G.G. Kovacs, TPPP/p25 in brain tumours: expression in non-neoplastic oligodendrocytes but not in oligodendroglioma cells, Acta Neuropathol 113 (2007) 213-215.

[25] G.G. Kovacs, L. László, J. Kovács, P.H. Jensen, E. Lindersson, G. Botond, T. Molnár, A. Perczel, F. Hudecz, G. Mezo, A. Erdei, L. Tirián, A. Lehotzky, E. Gelpi, H. Budka, and J. Ovádi, Natively unfolded tubulin polymerization promoting protein TPPP/p25 is a common marker of alpha-synucleinopathies, Neurobiol Dis. 17 (2004) 155-162.

[26] J. Ovádi, Moonlighting proteins in neurological disorders, IUBMB Life 63 (2011) 453-456.

[27] J. Oláh, A. Zotter, E. Hlavanda, S. Szunyogh, F. Orosz, K. Szigeti, J. Fidy and J. Ovádi, Microtubule assembly-derived by dimerization of TPPP/p25. Evaluation of thermodynamic parameters for multiple equilibrium system from ITC data, Biochim Biophys Acta 1820 (2012) 785-794.

[28] A. Zotter, A. Bodor, J. Oláh, E. Hlavanda, F. Orosz, A. Perczel and J. Ovádi, Disordered TPPP/p25 binds GTP and displays Mg(2+)-dependent GTPase activity, FEBS Lett 585 (2011) 803-808.

[29] A. Zotter, J. Oláh, E. Hlavanda, A. Bodor, A. Perczel, K. Szigeti, J. Fidy and J. Ovádi, Zn(2)+-induced rearrangement of the disordered TPPP/p25 affects its microtubule assembly and GTPase activity, Biochemistry 50 (2011) 9568-9578.

[30] D.E. Otzen, D.M. Lundvig, R. Wimmer, L.H. Nielsen, J.R. Pedersen and P.H. Jensen, p25alpha is flexible but natively folded and binds tubulin with oligomeric stoichiometry, Protein Sci 14 (2005) 1396-1409.

[31] S. Tabor and C.C. Richardson, A bacteriophage T7 RNA polymerase/promoter system for controlled exclusive expression of specific genes, Proc Natl Acad Sci U S A 82 (1985) 1074-1078.

[32] E.A. Bayer, E. Skutelsky and M. Wilchek, The avidin-biotin complex in affinity cytochemistry, Methods Enzymol 62 (1979) 308-315.

[33] C.N. Na and S.N. Timasheff, Interaction of vinblastine with calf brain tubulin: multiple equilibria, Biochemistry 25 (1986) 6214-6222.

[34] N. Tőkési, A. Lehotzky, I. Horváth, B. Szabó, J. Oláh, P. Lau and J. Ovádi, TPPP/p25 promotes tubulin acetylation by inhibiting histone deacetylase 6, J Biol Chem 285 (2010) 17896-17906.

[35] J.C. Louis, E. Magal, D. Muir, M. Manthorpe and S. Varon, CG-4, a new bipotential glial cell line from rat brain, is capable of differentiating in vitro into either mature oligodendrocytes or type-2 astrocytes, J Neurosci Res 31 (1992) 193-204.

[36] M.M. Bradford, A rapid and sensitive method for the quantitation of microgram quantities of protein utilizing the principle of protein-dye binding, Anal. Biochem. 72 (1976) 248-254.

[37] J.W. Meeusen, H. Tomasiewicz, A. Nowakowski and D.H. Petering, TSQ (6-methoxy-8-p-toluenesulfonamido-quinoline), a common fluorescent sensor for cellular zinc, images zinc proteins, Inorg Chem 50 (2011) 7563-7573.

[38] O.M. El-Agnaf, S.A. Salem, K.E. Paleologou, M.D. Curran, M.J. Gibson, J.A. Court, M.G. Schlossmacher and D. Allsop, Detection of oligomeric forms of alpha-synuclein protein in human plasma as a potential biomarker for Parkinson's disease, FASEB J 20 (2006) 419-425.

[39] H. Fukumoto, T. Tokuda, T. Kasai, N. Ishigami, H. Hidaka, M. Kondo, D. Allsop and M. Nakagawa, High-molecular-weight beta-amyloid oligomers are elevated in cerebrospinal fluid of Alzheimer patients, Faseb J 24 (2010) 2716-2726.

[40] A. Lehotzky, L. Tirián, N. Tőkési, P. Lénárt, B. Szabó, J. Kovács and J. Ovádi, Dynamic targeting of microtubules by TPPP/p25 affects cell survival, J Cell Sci 117 (2004) 6249-6259.

[41] O. Goldbaum, P.H. Jensen and C. Richter-Landsberg, The expression of tubulin polymerization promoting protein TPPP/p25alpha is developmentally regulated in cultured rat brain oligodendrocytes and affected by proteolytic stress, Glia 56 (2008) 1736-1746.

[42] F. Orosz, G.G. Kovács, A. Lehotzky, J. Oláh, O. Vincze and J. Ovádi, TPPP/p25: from unfolded protein to misfolding disease: prediction and experiments, Biol Cell 96 (2004) 701-711.

[43] T.G. Obrig, W.J. Culp, W.L. McKeehan and B. Hardesty, The mechanism by which cycloheximide and related glutarimide antibiotics inhibit peptide synthesis on reticulocyte ribosomes, J Biol Chem 246 (1971) 174-181.

[44] P. Zhou, Determining protein half-lives, Methods Mol Biol 284 (2004) 67-77.

[45] A. Iio, T. Takagi, K. Miki, T. Naoe, A. Nakayama and Y. Akao, DDX6 post-transcriptionally down-regulates miR-143/145 expression through host gene NCR143/145 in cancer cells, Biochim Biophys Acta 1829 (2013) 1102-1110.

[46] M.A. Mollah, S.C. Rakshit, K.S. Anwar, M.I. Arslan, N. Saha, S. Ahmed, K. Azad and T. Hassan, Zinc concentration in serum and cerebrospinal fluid simultaneously decrease in children with febrile seizure: findings from a prospective study in Bangladesh, Acta Paediatr 97 (2008) 1707-1711.

[47] J. Hardy and D. J. Selkoe, The amyloid hypothesis of Alzheimer's disease: progress and problems on the road to therapeutics, Science 297 (2002) 353-356.

[48] M. G. Spillantini, R. A. Crowther, R. Jakes, M. Hasegawa and M. Goedert, alpha-Synuclein in filamentous inclusions of Lewy bodies from Parkinson's disease and dementia with lewy bodies, Proc Natl Acad Sci U S A 95 (1998) 6469-6473.

[49] G. B. Irvine, O. M. El-Agnaf, G. M. Shankar and D. M. Walsh, Protein aggregation in the brain: the molecular basis for Alzheimer's and Parkinson's diseases, Mol Med 14 (2008) 451-464.

[50] S.P. Melo, K.W. Barbour and F.G. Berger, Cooperation between an intrinsically disordered region and a helical segment is required for ubiquitin-independent degradation by the proteasome, J Biol Chem 286 (2011) 36559-36567.

[51] M.J. Suskiewicz, J.L. Sussman, I. Silman and Y. Shaul, Context-dependent resistance to proteolysis of intrinsically disordered proteins, Protein Sci 20 (2011) 1285-1297.

[52] P. Tsvetkov, N. Myers, O. Moscovitz, M. Sharon, J. Prilusky and Y. Shaul, Thermo-resistant intrinsically disordered proteins are efficient 20S proteasome substrates, Mol Biosyst 8 (2012) 368-373.

9. FIGURE LEGENDS

Figure 1. Zinc binding to TPPP/p25 and dimerization-dependent effect of zinc on TPPP/p25-induced tubulin assembly. A: *Fluorescence spectroscopy using TSQ as specific zinc sensor*. Excitation wavelength was 360 nm, emission spectra were recorded at room temperature in PBS buffer. 20 μM TSQ without (solid line) or with 5 μM $ZnCl_2$ (bold line) and 5 μM TPPP/p25 (dashed line). The spectrum of TPPP/p25 (dotted line) and the effect of 5 μM $MnCl_2$ (dash-dot-dotted line) on the TSQ-$ZnCl_2$-TPPP/p25 complex are also shown. Three-five independent experiments were recorded. Representative spectra are shown; error of determinations (SEM) is ± 10%. B: *Turbidimetry.* The polymerization of tubulin was induced by addition of TPPP/p25 from a stock solution (400 μM) in the absence (bold line) or presence (dashed line) of $ZnCl_2$; or TPPP/p25 was diluted and incubated in the cuvette in the absence (solid line) and presence (dotted line) of $ZnCl_2$, then the reaction was initiated by addition of tubulin from a stock solution (280 μM) in polymerization buffer. In both sets of experiments the final concentrations of zinc, tubulin and TPPP/p25 were 100 μM, 7 μM and 3 μM, respectively. Three independent experiments were performed. Representative polymerization is shown; error of determinations (SEM) is ± 10%. C and D: *Sandwich ELISA. Effects of divalent metal ions on the monomer-dimer equilibrium of TPPP/p25 at different conditions.* Monoclonal anti-TPPP/p25 antibody was immobilized on the plate, and TPPP/p25 at different concentrations was added onto the plate without or with divalent cations (2 or 10 μM). In the case of incubation, TPPP/p25 was pre-incubated with or without 100 μM DTE for 30 min at room temperature. Then the same monoclonal anti-TPPP/p25 antibody was added in biotinylated form, which was detected through peroxidase conjugated avidin reaction. C: The effect of incubation and/or metal ions on TPPP/p25 at 1.25 (black column) or 0.3125 (white column) μM protein concentration. * Significant difference between samples and the control at the same TPPP/p25 concentration (according to the Student's t-test, $p < 0.05$). D: TPPP/p25 without (●, bold line) or with incubation with DTE (○, solid line), in the presence of 2 μM $ZnCl_2$ without (▲, dashed line) or with incubation with DTE (△, dotted line). Error bars represent the standard error of the determinations (SEM) (n = 3) (C, D).

Figure 2. Global overview of intracellular TPPP/p25 level (red) in the CHO10 cell populations visualized by confocal fluorescence microscopy. Control (induced, no zinc) and zinc-treated cells. TPPP/p25 expression was induced by 100 ng/mL doxycycline (overnight), then the cells were treated with 10 μM Zn^{2+} for 3 hours. Nuclei were counterstained with DAPI (blue). Scale bar: 125 μm.

Figure 3. Effect of zinc and/or vinblastine (VBL) on the localization and level of TPPP/p25 in CHO10 cells. A: Confocal fluorescence microscopic images using anti-TPPP/p25 antibody. Nuclei were counterstained with DAPI (blue). Scale bar: 10 μm. B: Quantification of the intracellular TPPP/p25 level in the absence (grey column) and presence (white column) of zinc and/or VBL in CHO10 cells by cELISA.

TPPP/p25 expression was induced by 100 ng/mL doxycycline (overnight), then the cells were treated with 10 μM Zn^{2+} and/or 1 μM VBL for 3 hours. Error bars represent the standard error of the determinations (SEM) (n = 3). * Significant difference between samples with and without the addition of zinc (according to the Student's t-test, $p < 0.05$).

Figure 4. The effect of zinc on the intracellular TPPP/p25 level in CHO10 cells at different TPPP/p25 expression levels as determined by cELISA. A: TPPP/p25 expression was induced by doxycycline as described in Materials and Methods. B: Effect of addition of 0 (black column), 5 (grey column) or 10 (white column) μM $ZnCl_2$ at different expression levels of TPPP/p25 were determined after 3 hours of incubation. Error bars represent the standard error of the determinations (SEM) (n = 3). * Significant difference between samples with and without the addition of zinc (according to the Student's t-test, $p < 0.05$).

Figure 5. Effect of inhibition of protein synthesis by cycloheximide (CI) on the zinc-induced elevation of the intracellular TPPP/p25 level determined by immunoblotting (A) and quantified by densitometry using ImageJ 1.42 (shown in B). Doxycycline induction (Lane 5), CI treatment in the absence (Lane 1-2, from parallel samples) and presence of zinc (Lane 3-4, from parallel samples). TPPP/p25 expression was induced by 100 ng/mL doxycycline (overnight), then the cells were treated with 20 μg/mL CI and/or 10 μM Zn^{2+} as described in the Materials and Methods. GAPDH was used as loading control.

Figure 6. Quantification of the effect of Zn^{2+} on the intracellular TPPP/p25 level in CHO10 cells at different expression levels. The TPPP/p25 level was determined by cELISA as described in the Materials and Methods. The TPPP/p25 expression level was modulated with MG132 (grey columns) or with cycloheximide block (CI, black columns) treatments. TPPP/p25 expression was induced by 100 ng/mL doxycycline (overnight), then the cells were treated with 20 μg/mL CI and/or 10 μM Zn^{2+} and/or 10 μM MG132 as described in the Materials and Methods. Error bars represent the standard error of the determinations (SEM) (n = 3). * Significant difference between samples with and without the addition of zinc and/or MG132 (according to the Student's t-test, $p < 0.05$).

Figure 7. Effect of Zn^{2+} on the endogeneous expression of TPPP/p25 in living CG-4 cells. The images of the cells at two different amplification are shown obtained by immunofluorescence microscopy using monoclonal anti-tubulin (green) and anti-TPPP/p25 (red) antibodies. The cells were treated with 1 μM Zn^{2+}. Nuclei were counterstained with DAPI (blue). Scale bar: 12.5 μm (A) and 5 μm (B).

Figure 1
Click here to download high resolution image

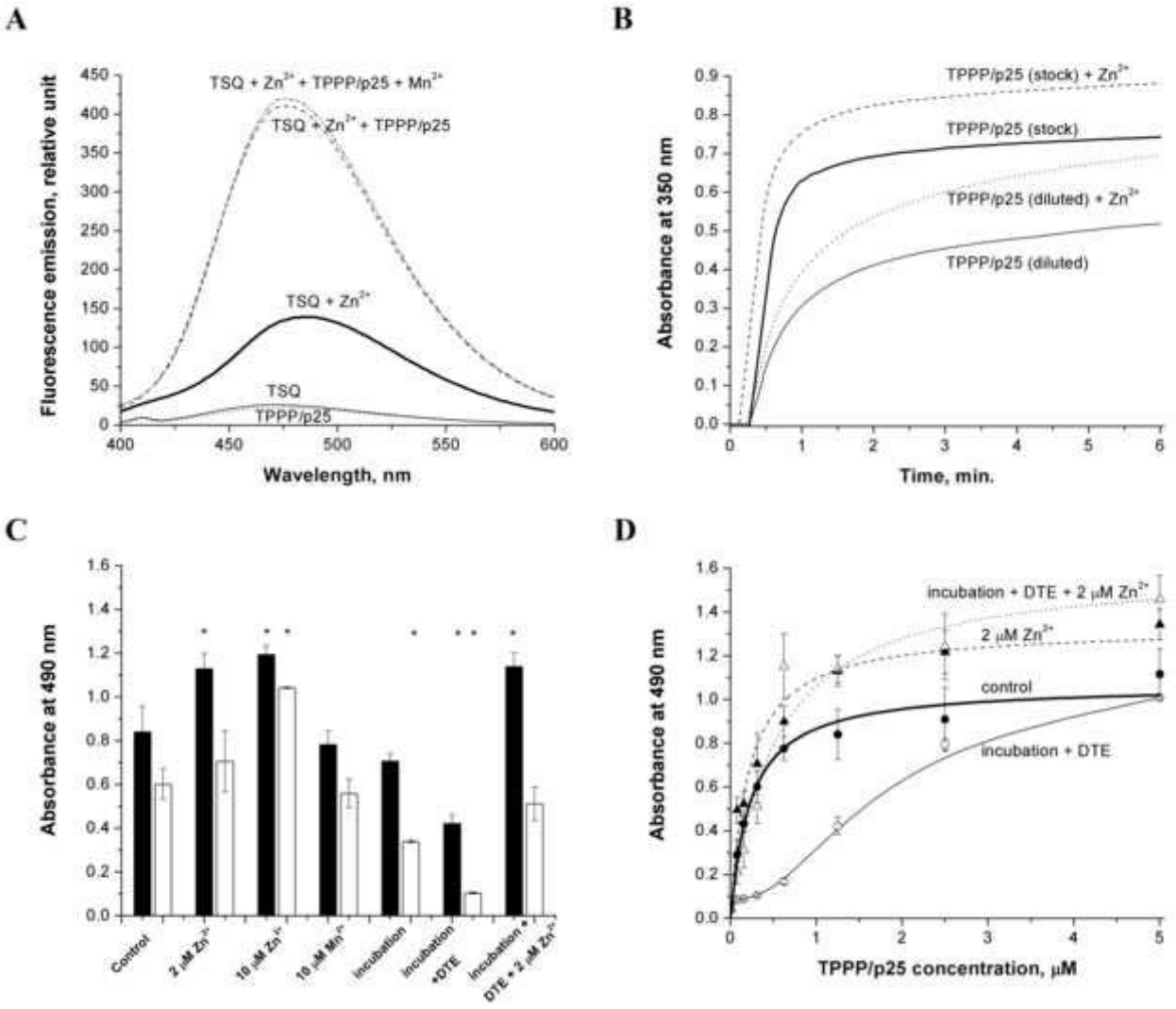

Figure 2
Click here to download high resolution image

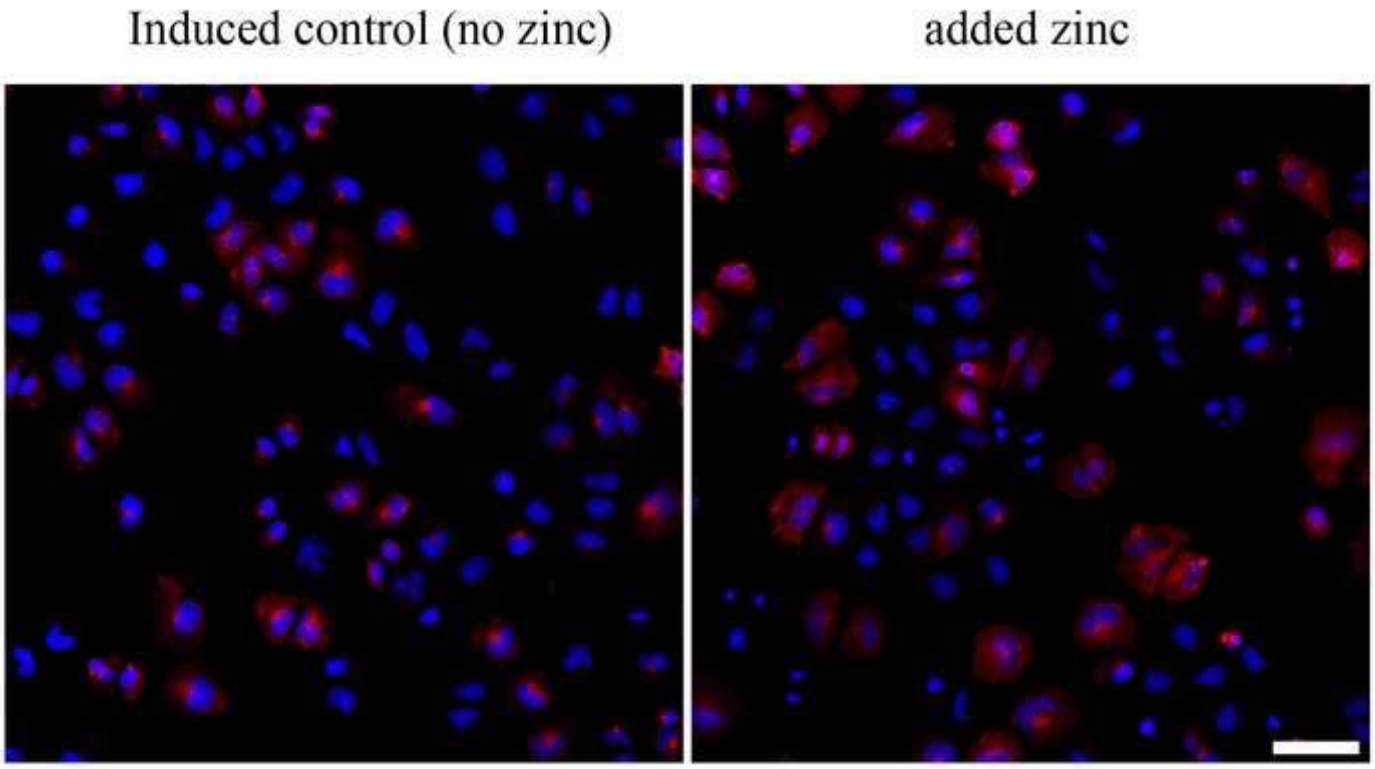

Figure 3
Click here to download high resolution image

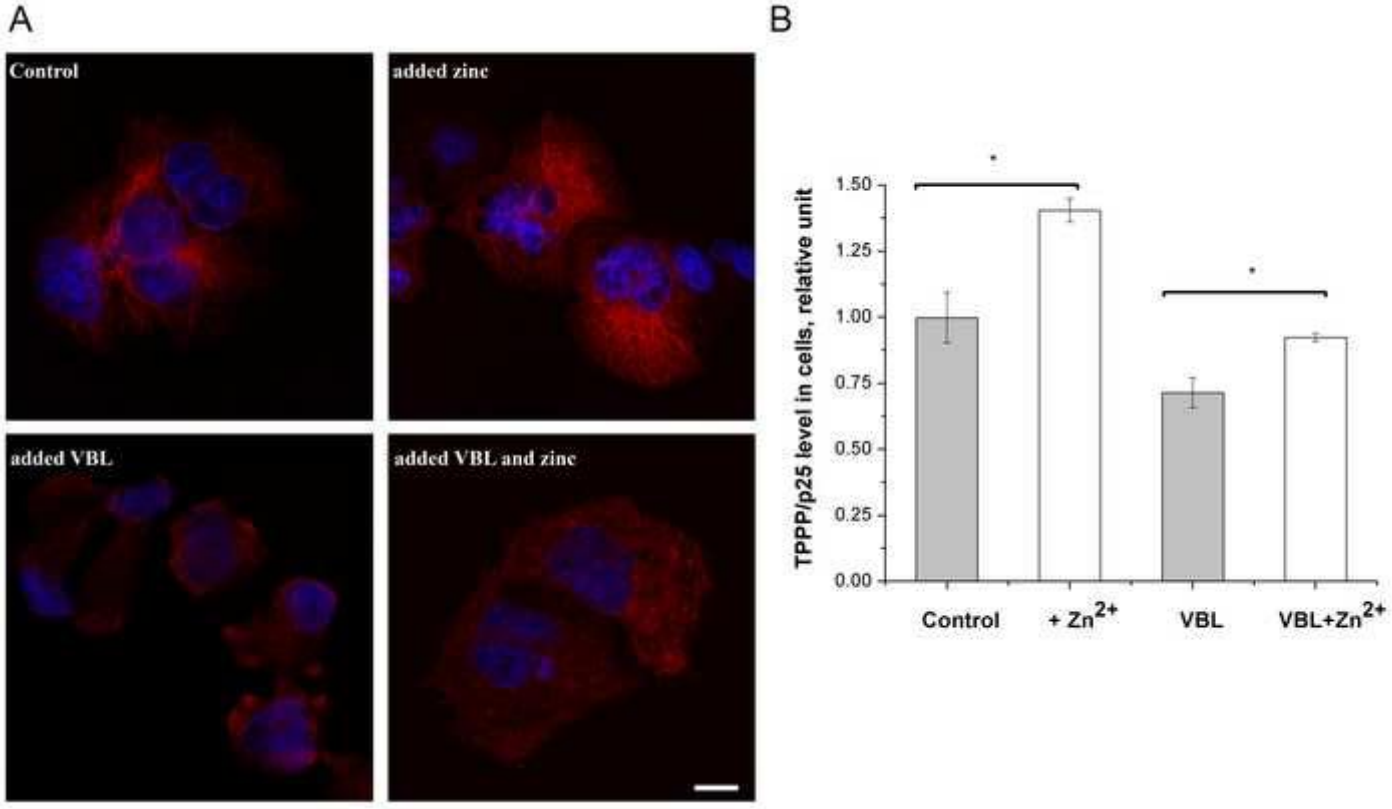

Figure 4
Click here to download high resolution image

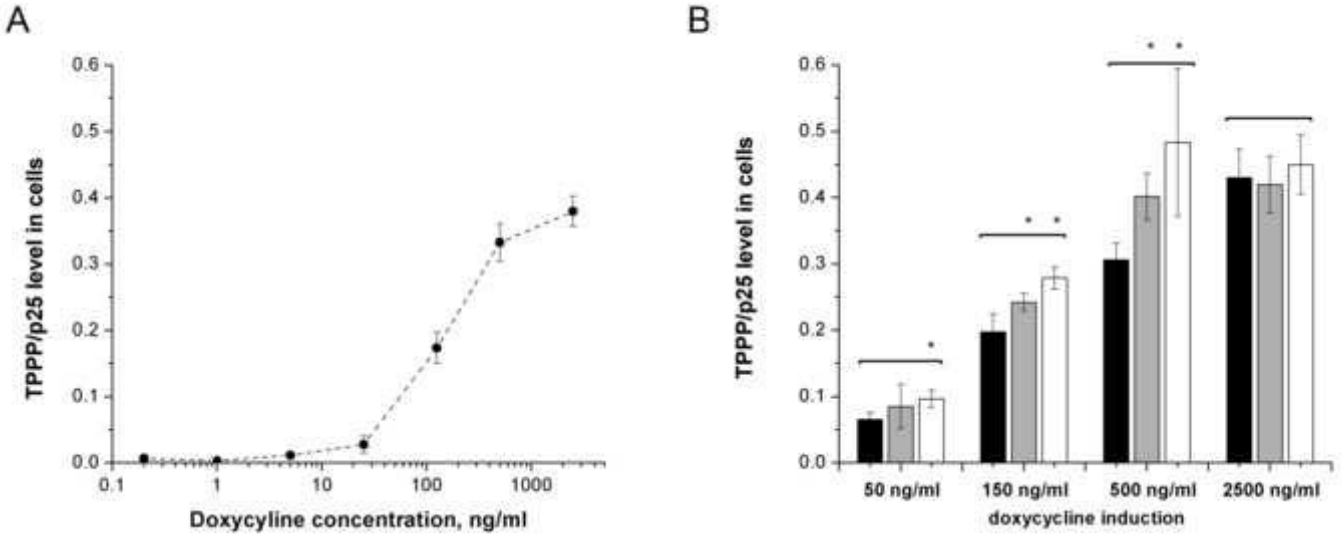

Figure 5
Click here to download high resolution image

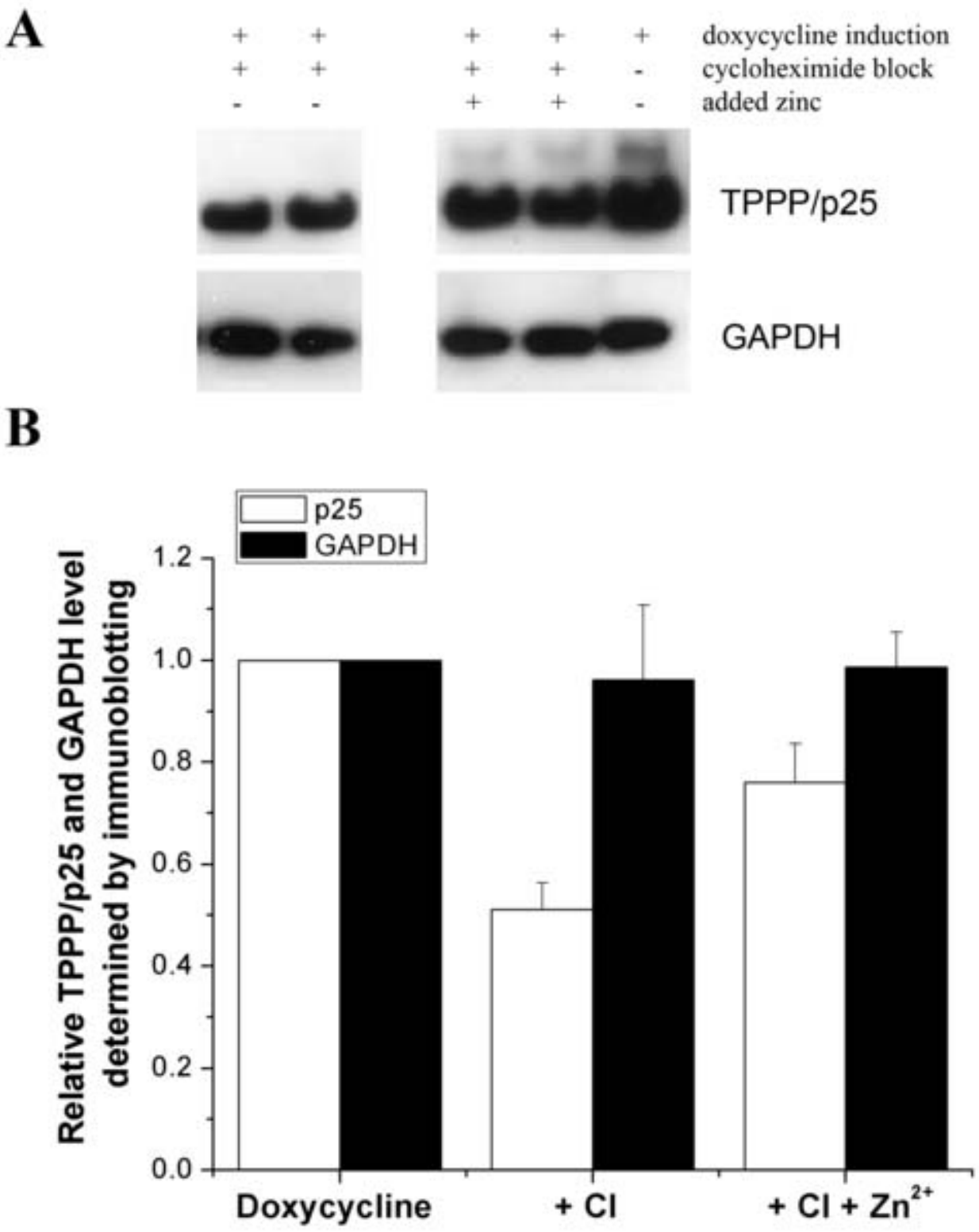

Figure 6
Click here to download high resolution image

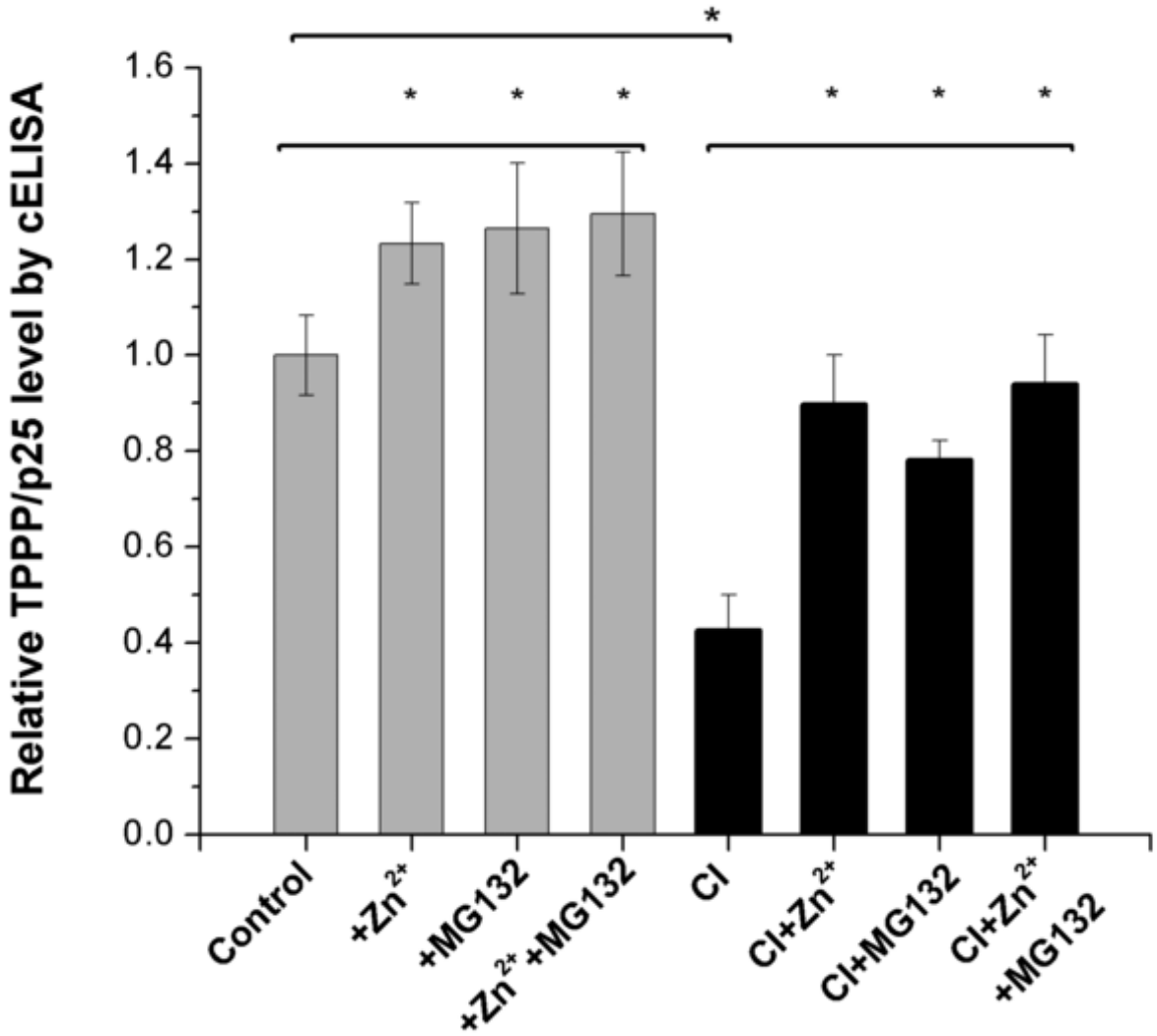

Figure 7
Click here to download high resolution image